Solid State Ionics 309 (2017) 187–191

Contents lists available at ScienceDirect

Solid State Ionics

journal homepage: www.elsevier.com/locate/ssi

Proton diffusion mechanisms in the double perovskite cathode material $GdBaCo_2O_{5.5}$: A molecular dynamics study

Fabien Brieuc[a,*], Guilhem Dezanneau[a], Marc Hayoun[b], Hichem Dammak[a,b]

[a] Laboratoire Structures, Propriétés et Modélisation des Solides, CentraleSupélec/CNRS, Université Paris-Saclay, Grande voie des vignes, 92295 Chatenay-Malabry Cedex, France

[b] Laboratoire des Solides Irradiés, École Polytechnique/CEA/CNRS, Université Paris-Saclay, 91128 Palaiseau, France

ARTICLE INFO

Keywords:
PCFC
Proton conductor
Double perovskite
Mixed conductivity
Molecular dynamics

ABSTRACT

$GdBaCo_2O_{5+x}$ compounds have demonstrated to be very efficient cathode materials not only in solid oxide fuel cells but also in proton conducting fuel cells. In this last case, the excellent properties could be due to the presence of mixed electron-proton conduction. We study here the diffusion of the proton in this material using molecular dynamics simulations. Two different diffusion mechanisms are observed. The predominant mechanism is the standard proton transfer between two neighbouring oxygen atoms combined with the rotation of H around its first neighbour oxygen atom. The second mechanism consists in the migration of the OH group where both oxygen and hydrogen atoms diffuse together. Strong spatial correlations between successive proton jumps are evidenced. This is likely related to the presence of oxygen vacancies and to the concerted diffusion of hydrogen and oxygen atoms.

1. Introduction

Since the first article on the use of $GdBaCo_2O_{5+x}$ double perovskite compounds as cathode materials in solid oxide fuel cells [1] and the exhaustive study of their properties by A. Tarancón and co-authors [2–5], the interest for this family of compounds has been growing. This interest principally comes from the excellent properties, in particular the Area Specific Resistance (ASR), observed for this material as an air electrode material. For example, an ASR of 0.25 $\Omega.cm^2$ has been measured at 625 °C [2]. Several attempts have been made to improve the chemical stability, the thermal expansion coefficient (too high in the pristine compound) and the electrochemical properties. The main pathways of improvement have consisted in the substitution of Ba by Sr, leading to potentially more stable compounds [6–8], and the use of other transition metals to decrease the thermal expansion [8–11]. A conclusion from these studies is that increasing the chemical stability and lowering the thermal expansion coefficient is possible but most often leads to a decrease of electrochemical performance. Besides these experimental results, theoretical studies have provided a deeper understanding of the atomic scale mechanisms of diffusion in this type of compound. In particular, Molecular Dynamics (MD) simulations have led to the confirmation of the 2D nature of the oxygen diffusion in $REBaCo_2O_{5.5}$ compounds (RE = La, Pr, Gd, Y, …) and have revealed the associated diffusion mechanisms [12,13]. It has been shown through neutron diffraction analysis combined with MD calculations that long range diffusion occurs through oxygen ion jumps between gadolinium (GdO) and cobalt (CoO_2) planes, thus emphasising the importance of the presence of oxygen vacancies in the CoO_2 plane [14].

More recently, these double perovskite compounds have been applied in Proton Conducting Fuel Cells (PCFCs), displaying excellent properties [15]. For instance, in La-doped $GdBaCo_2O_{5+x}$, it was shown using electrode polarization resistance that the apparent activation energy decreases from around 1.3 eV at high temperatures to around 0.5 eV below 550 °C [16]. This was attributed essentially to a change from oxygen ion transport at high temperatures to mainly proton transport at low temperatures. This assumption was supported by thermogravimetric measurements showing a weight increase under wet atmospheres for the La-doped compounds.

As shown in a recent article, $PrBaCO_2O_{5+x}$ used as electrode material presents a much lower ASR in wet atmosphere compared to dry atmosphere [17]. This result is potentially linked with the incorporation of water inside the double cobaltite compound, incorporation that would favor the oxygen reduction reaction, even if there is no direct proof of proton incorporation in this material. A previous study also showed that $REBaCo_2O_{5+x}$ double perovskites are stable in humid atmospheres and potentially incorporate water at low temperatures [18]. Nevertheless, recent neutron diffraction experiments did not confirm the presence of water in humidified $NdBaCo_2O_{5+x}$ at high temperatures

* Corresponding author.
E-mail address: fabien.brieuc@centralesupelec.fr (F. Brieuc).

http://dx.doi.org/10.1016/j.ssi.2017.07.017
Received 15 March 2017; Received in revised form 20 June 2017; Accepted 24 July 2017
Available online 04 August 2017

[19]. However, DFT calculations found either exothermic or endothermic hydration of $GdBaCo_2O_{5.5}$ depending on the original structure considered [20]. These calculations also seem to indicate a preferential location of protons close to CoO_2 and GdO planes [20]. Further experimental and theoretical studies are thus needed to investigate the possible hydration of double perovskite cobaltite compounds and to understand its effects on transport and electrochemical properties.

Keeping in mind that the hydration of a double cobaltite compound is still the object of debate, we assume in the present study a partial hydration, and performed MD simulations to understand proton diffusion mechanisms in $GdBaCo_2O_{5.5}$ and the role of hydration on transport properties.

2. Computation details

For the present study, the interatomic potentials within $GdBaCo_2O_{5.5}$ are those previously used to study oxygen diffusion in this material [12,13]. These potentials have proven their validity for reproducing oxygen sublattice dynamics [12,13]. Since proton transport is essentially a phonon-assisted process, through oxygen vibrations, all the ingredients are present for reproducing the proton diffusion in double cobaltites. The Buckingham potentials between the first neighbouring oxygen ion of the proton and the other cations were adapted to take into account the smaller charge on the oxygen atom of the hydroxyl group, following a procedure presented by Sierka et al. [21]. The proton transfer between the two first neighbouring oxygen atoms is described by the empirical valence bond (EVB) model, as originally presented by Raiteri et al. for proton conductors [22,23]. In particular, using this model, the proton diffusion coefficient is correctly reproduced in Y-doped barium zirconate as compared to experimental values [22]. The EVB parameters associated with the interactions between the proton and the other ions were taken from the original article on Y-doped $BaZrO_3$ [22]. All the parameters of the interatomic potentials are provided as Supplementary data.

The size of the MD simulation box was $6a \times 6b \times 3c$ as compared to the original double perovskite cell, containing 108 Ba, 108 Gd, 216 Co and 594 O, corresponding to the formula $GdBaCo_2O_{5.5}$ (GBCO). In the initial configuration, the GdO plane is deficient in oxygen atoms with respect to the stoichiometric double perovskite structure. The associated empty sites represent oxygen vacancies, which can migrate during the MD simulations. One proton is introduced in the simulation box and the electrical neutrality is ensured by adding a uniform background charge. The simulations were performed with a time step of 0.3 fs in the NVT ensemble using a Langevin thermostat [24] and at a pressure close to zero. The temperature was varied between 1200 and 1900 K and average quantities were obtained using equilibrium trajectories of 11 ns to 2 ns, respectively. All the computations were carried out with a homemade code.

3. Results

Simulations first indicate that the presence of one proton out of 1026 atoms does not affect the volume of the cell. As shown in previous studies [12,13,25], oxygen atoms diffuse parallel to the (*a*,*b*) plane but are blocked in the *c* direction. Up to 1700 K, BaO planes act as barriers for the diffusion of oxygen atoms, which explains their limited displacement in the *c* direction and thus the 2D nature of the diffusion. The oxygen diffusion pathway is composed of a sequence of jumps between the GdO plane and an adjacent CoO_2 plane, similarly to what have been previously obtained in GBCO [12,13,25] and observed experimentally in a similar compound ($NdBaCo_2O_{5+x}$) [14,26].

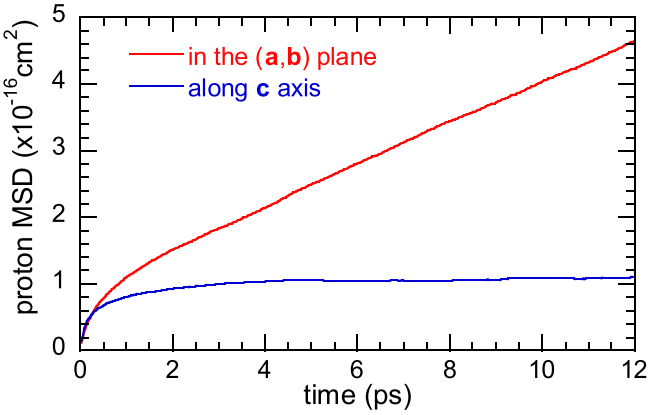

Fig. 1. Mean Square Displacement (MSD) of a proton in GBCO at 1700 K.

The Mean Square Displacement (MSD) of the proton as obtained from simulations at 1700 K is given in Fig. 1. The proton diffuses in parallel to the (*a*,*b*) plane and is blocked in the *c* direction, similarly to the oxygen atoms. Fig. 2 shows the diffusion coefficient in the (*a*,*b*) plane of both protons and oxygen atoms as extracted from MSD. Comparison is made with previous experimental and theoretical results, which are only available for oxygen. The calculated oxygen diffusion coefficient is in reasonable agreement with experiments [3]. For the first time, the proton diffusion coefficient (blue squares in Fig. 2) is evaluated in GBCO. It is found to be more than one order of magnitude higher than that of oxygen. Furthermore, the activation energy associated with proton diffusion (0.71 ± 0.03 eV) is found to be lower than the activation energy for oxygen diffusion (1.01 ± 0.03 eV). This difference of activation energy between oxygen and proton migration is commonly observed in perovskite [28–32] or other oxide compounds [33,34]. For instance, in Y-doped barium zirconate, an activation energy of 0.95 eV [31] is reported for oxygen ion migration, while it is 0.40–0.45 eV [28–32] for the proton migration.

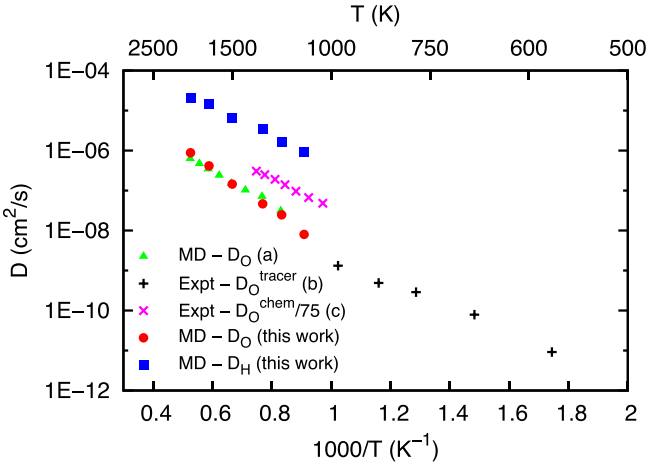

Fig. 2. Proton (full squares) and oxygen (full circles) diffusion coefficients in the (*a*,*b*) plane, D (in log scale), as obtained from MD simulations. Previous oxygen results in GBCO are also displayed: (a) MD simulations [12], (b) from oxygen exchange [3] and (c) from conductivity relaxation [27,13]. (For interpretation of the references to color in this figure, the reader is referred to the web version of this article.)

Unfortunately, no data are available concerning proton diffusion/conductivity in double perovskite cobaltites which could be compared

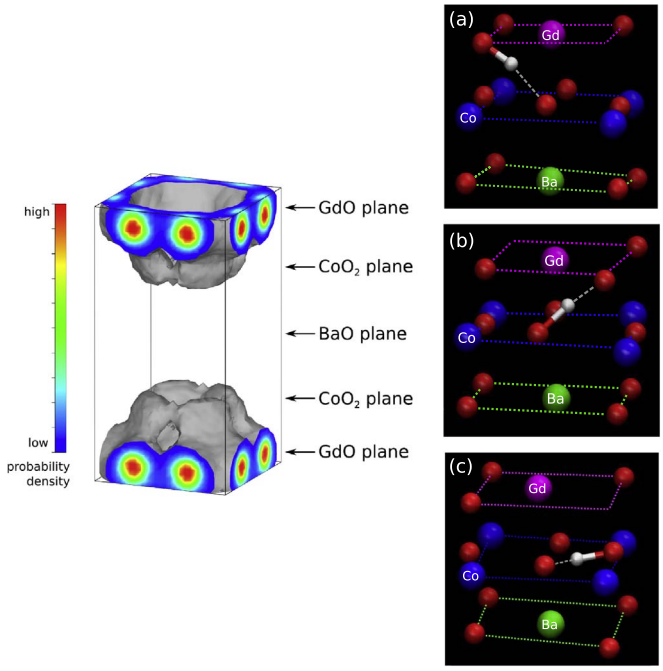

Fig. 3. Left - probability density map of the proton in GBCO at 1500 K, obtained from MD trajectories. Right – snapshots of the preferential locations of the proton in GBCO (*i.e.* configurations associated with the probability density maximums).

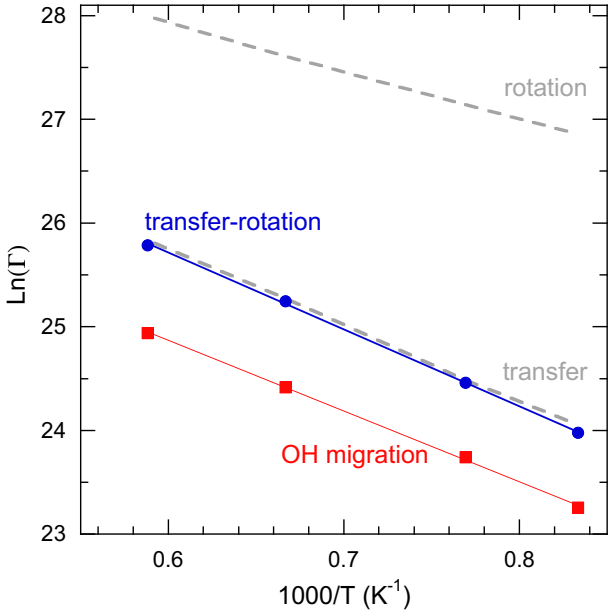

Fig. 4. Arrhenius plot of the frequency, Γ (Hz), of the transfer-rotation (full circles), and OH migration (full squares) mechanisms associated to the diffusion of the proton. Pure rotation and transfer events are also shown (grey dashed lines).

to our simulation results. This comes from the fact that proton incorporation through water uptake is difficult to evaluate in electrode materials due to the concomitant oxygen uptake (oxidation reaction). We consider that one method could nevertheless be used, namely nuclear reaction analysis, which would allow the quantification of proton presence inside dense GBCO materials, for concentrations varying from traces to a few percent [35]. This method would not have the drawbacks of thermogravimetry measurements and could give a direct proof of proton incorporation. If the incorporation of protons is confirmed, the proton diffusion coefficient could be evaluated through methods like TOF-SIMS (Time-of-Flight Secondary Ion Mass Spectrometry) which has been applied with success in lanthanum tungstates [36], keeping in mind that this may provide information on water diffusion rather than on proton diffusion.

Before the analysis of the proton migration mechanisms, let us consider its preferential locations in GBCO. The density map on Fig. 3 (left) indicates that the proton is essentially located slightly above or below the GdO plane and to a less extent close to the CoO_2 plane. The proton is likely to be rejected from the BaO plane just like oxygen vacancies. Indeed, at 1500 K, 97% of the oxygen vacancies are, at equilibrium, located in GdO planes, while the remaining 3% are in CoO_2 planes. In other words, the proton is never bonded to an oxygen atom of the BaO plane. The snapshots of Fig. 3 (right), represents the preferential locations of the proton. Most of the time (87% at 1500 K), the proton is bonded to an oxygen of the GdO plane (snapshot (a)) while the rest of the time it is bonded to an atom of the CoO_2 plane (snapshots (b) and (c)).

From the density map of Fig. 3, the proton diffuses within the same GdO and CoO_2 planes since the probability density is zero near the in-between BaO plane. This corroborates the bidimensional nature of proton diffusion parallel to the (*a*,*b*) plane (see Fig. 1). The diffusion of protons in GBCO follows a scheme where the proton is successively bonded to one oxygen atom of the GdO plane and then to an oxygen atom of the CoO_2 plane. Moreover, the OH bond most of the time points in a direction that keeps the proton between the GdO and the CoO_2 planes. This explains the high density of protons observed between these two planes.

The analysis of the MD trajectories shows that the long-range migration of the proton is obtained through two mechanisms.

i) The proton transfer between the two neighbouring oxygen atoms (Grotthuss mechanism) combined with the rotation of H around its first neighbour oxygen atom. The limiting step is the proton transfer as shown in Fig. 4. The activation energies are equal to 0.63 and 0.38 eV for the proton transfer and rotation, respectively. Accounting for the two types of events, the time of flight of the transfer-rotation mechanism is almost fully given by that of the transfer step which is around 0.1 ps. In addition, proton transfer between GdO and CoO_2 planes represents around 93% of the total number of transfer events at T = 1500 K, the others being within the CoO_2 plane (7%).
ii) The second mechanism consists in the migration of the whole OH group (vehicle mechanism [32]) which occurs mainly along ⟨101⟩ directions of the cubic cell. The corresponding time of flight is about 0.3 ps. At 1500 K, the contributions of the two diffusion mechanisms, transfer-rotation and OH migration, are 70% and 30%, respectively. Fig. 4 shows the Arrhenius plot of their associated jump frequencies. The extracted activation energies are very similar, being equal to 0.64, and 0.59 eV for the transfer-rotation and OH migration mechanisms, respectively.

These activation energies are much smaller than the ones calculated from the diffusion coefficient values obtained using the Mean Square Displacement. This can be explained by the presence of spatial correlations between successive jumps leading to a proton diffusion that cannot be described by a purely random walk. The deviation from a purely Brownian diffusion can be quantified using the correlation factor, f [37,38], which is estimated using the jump frequencies of the transfer-rotation (Γ_H) and of the OH-migration (Γ_{OH}) events. In contrast

to a purely random walk, for which $f = 1$, the jump directions in GBCO may not be equally probable and may depend on the prior jump. The jump sequence is thus correlated and $f \neq 1$.

The proton diffusion in GBCO is considered in the (a,b) plane since the H atom never visits the BaO plane. The correlation factor is defined as the ratio between the MSD diffusion coefficient, D_H, and the diffusion coefficient estimated from the jump frequencies in the purely random walk regime:

$$f = \frac{D_H}{\frac{1}{4}(\Gamma_H d_H^2 + \Gamma_{OH} d_{0H}^2)}$$

where the factor 1/4 comes from the 2D nature of the diffusion.

The jump frequency Γ_H corresponds to the transfer-rotation combination [39]:

$$\frac{1}{\Gamma_H} = \frac{1}{\Gamma_{rotation}} + \frac{1}{\Gamma_{transfer}}$$

and Γ_{OH} is associated to the OH migration mechanism where both oxygen and hydrogen atoms migrate together. The jump lengths d_H and d_{OH} are the proton displacements projected in the (a,b) plane. Both lengths are about $a/2$, since the jumps are oriented mainly along the [101] or [011] directions in the cubic cell. Our MD values for the correlation factor are equal to 0.28, 0.59, and 0.76 at 1300 K, 1500 K, and 1700 K, respectively. These values less than unity mean that there exists a strong spatial correlation between the jumps. This is likely due to the presence of oxygen vacancies and to the concerted diffusion of oxygen and hydrogen atoms (vehicle diffusion). Indeed, we obtained a correlation factor close to 1 (0.94) in the case of a proton diffusion in $BaZrO_3$ where the oxygen atoms do not migrate. This temperature-dependent correlation factor may explain in part the high activation energy of the proton migration observed here.

Besides giving some features of the proton diffusion mechanisms, these results provide some evaluation of the potential influence of hydration of GBCO on its transport properties. Indeed, if we consider for instance the filling of 5% of the oxygen vacancies in $GdBaCo_2O_{5.5}$, we would have a conductivity for protons at 600 °C that is 0.5 times that of oxygen ions. In other words, a slight incorporation of protons in GBCO would result in a high proton conductivity at the working temperature of PCFCs *i.e.* ~600 °C.

4. Conclusions

Using a reactive-force field, we have been able to treat the potential diffusion of protons in GBCO. We have shown that protons would present a 2D diffusion, analogous to that of oxygen in this material. We evaluated the proton diffusion coefficient being more than one order of magnitude greater than the oxygen diffusion coefficient. We also show that the activation energy of the 2D proton diffusion is equal to 0.71 eV, smaller than for the oxygen atoms. By analysing the trajectories, we found that protons jump from oxygen atoms in the GdO plane to oxygen atoms in the CoO_2 plane and reciprocally. The OH bond points in a direction that keeps the proton between the GdO and CoO_2 planes. This corresponds to the prevailing diffusion mechanism where a proton transfer (Grotthuss mechanism) between the two neighbouring oxygen atoms is combined with a rotation of H around its first neighbour oxygen atom. A second mechanism (vehicle mechanism) consists in the migration of the OH group where both oxygen and hydrogen atoms migrate together, mainly along ⟨101⟩ directions of the cubic cell. These two mechanisms have similar activation energies around 0.6 eV. We also evidenced a strong spatial correlation of the atomic jumps, since a correlation factor less than unity was found in the temperature range 1300–1700 K. This correlation seems to be linked to the concerted diffusion of hydrogen and oxygen atoms.

These results are important because they predict a high proton diffusion coefficient in hydrated double perovskite cobaltite compounds, which would strongly help the cathode reaction in PCFCs. Further experiments are nevertheless needed to quantify the hydration degree of these compounds. We estimate that a partial filling by water of 5% of the oxygen vacancies in GBCO would lead to a proton conductivity at 600 °C comparable to that of oxygen ions. For further work, a detailed comparison of the proton diffusion in double perovskite compounds, such as GBCO, and in more standard perovskites, such as $BaZrO_3$, could give important information on the differences between these two classes of materials.

Acknowledgements

This work was performed using HPC resources from the *mesocentre* computing center of CentraleSupélec, which is supported by CentraleSupélec and CNRS.

Appendix A. Supplementary data

Supplementary data to this article can be found online at http://dx.doi.org/10.1016/j.ssi.2017.07.017.

References

[1] A. Chang, S.J. Skinner, J.A. Kilner, Solid State Ionics 177 (2006) 2009–2011.
[2] A. Tarancón, A. Morata, G. Dezanneau, S.J. Skinner, J.A. Kilner, S. Estradé, F.H. Hernandez-Ramírez, F. Peiró, J.R. Morante, J. Power Sources 174 (2007) 255–263.
[3] A. Tarancón, S.J. Skinner, F. Hernandez-Ramirez, J.A. Kilner, J. Mater. Chem. 17 (2007) 3175–3181.
[4] A. Tarancón, D. Marrero-López, J. Peña-Martínez, J.C. Ruiz-Morales, P. Núñez, Solid State Ionics 179 (2008) 611–618.
[5] A. Tarancón, J. Peña-Martínez, D. Marrero-López, A. Morata, J.C. Ruiz-Morales, P. Núñez, Solid State Ionics 179 (2008) 2372–2378.
[6] H. Ding, X. Xue, J. Alloys Compd. 496 (2010) 683–686.
[7] X. Zhang, M. Jin, J. Power Sources 195 (2010) 1076–1078.
[8] J.H. Kim, J.T.S. Irvine, Int. J. Hydrog. Energy 37 (2012) 5920–5929.
[9] Y. Hu, C. Bogicevic, Y. Bouffanais, M. Giot, O. Hernandez, G. Dezanneau, J. Power Sources 242 (2013) 50–56.
[10] A. Kulka, Y. Andrzej, G. Dezanneau, J. Molenda, Funct. Mater. Lett. 4 (2011) 157–160.
[11] X.L. Che, Y. Shen, H. Li, T. He, J. Power Sources 222 (2013) 288–293.
[12] J. Hermet, G. Geneste, G. Dezanneau, Appl. Phys. Lett. 97 (2010) 174102.
[13] J. Hermet, B. Dupé, G. Dezanneau, Solid State Ionics 216 (2012) 50–53.
[14] Y. Hu, O. Hernandez, T. Broux, M. Bahout, J. Hermet, A. Ottochian, C. Ritter, G. Geneste, G. Dezanneau, J. Mater. Chem. 22 (2012) 18744–18747.
[15] B. Lin, S. Zhang, L. Zhang, L. Bi, H. Ding, X. Liu, J. Gao, G. Meng, J. Power Sources 177 (2008) 330–333.
[16] R. Strandbakke, V.A. Cherepanov, A.Y. Zuev, D.S. Tsvetkov, C. Argirusis, G. Sourkouni, S. Prünte, T. Norby, Solid State Ionics 278 (2015) 120–132.
[17] A. Grimaud, J.-M. Bassat, F. Mauvy, M. Pollet, A. Wattiaux, M. Marrony, J.-C. Grenier, J. Mater. Chem. A 2 (2014) 3594–3604.
[18] G. Goupil, T. Delahaye, B. Sala, F. Lefebvre Joud, G. Gauthier, Solid State Ionics 263 (2014) 15–22.
[19] M. Bahout, S.S. Pramana, J.M. Hanlon, V. Dorcet, R.I. Smith, S. Paofai, S.J. Skinner, J. Mater. Chem. A 3 (2015) 15420–15431.
[20] E. Coulaud, G. Dezanneau, G. Geneste, J. Mater. Chem. A 3 (2015) 23917–23929.
[21] M. Sierka, J. Sauer, Faraday Discuss. 106 (1997) 41–62.
[22] P. Raiteri, J.D. Gale, G. Bussi, J. Phys. Condens. Matter 23 (2011) 334213.
[23] A. Ottochian, G. Dezanneau, C. Gilles, C. Knight, P. Raiteri, J.D. Gale, J. Mater. Chem. A 2 (2014) 3127–3133.
[24] M. Binggeli, J.R. Chelikowsky, Phys. Rev. B 50 (1994) 11764.
[25] D. Parfitt, A. Chroneos, A. Tarancón, J.A. Kilner, J. Mater. Chem. 21 (2011) 2183–2186.
[26] R.A. Cox-Galhotra, A. Huq, J.P. Hodges, J.-H. Kim, C. Yu, X. Wang, A.J. Jacobson, S. McIntosh, J. Mater. Chem. A 1 (2013) 3081–3100.
[27] M.-B. Choi, S.-Y. Jeon, J.-S. Lee, H.-J. Hwang, S.-J. Song, J. Power Sources 195 (2010) 1059–1064.
[28] K. Wakamura, J. Phys. Chem. Solids 66 (2005) 133–142.
[29] S. Ricote, N. Bonanos, A. Manerbino, W.G. Coors, Int. J. Hydrog. Energy 37 (2012) 7954–7961.

[30] S. Ricote, N. Bonanos, H.J. Wang, B.A. Boukamp, Solid State Ionics 213 (2012) 36–41.
[31] A.C.T. van Duin, B.V. Merinov, S.S. Han, C.O. Dorso, W.A. Goddard III, J. Phys. Chem. A 112 (2008) 11414–11422.
[32] K.-D. Kreuer, Annu. Rev. Mater. Res. 33 (2003) 333–359.
[33] Y. Larring, T. Norby, Solid State Ionics 77 (1995) 147–151.
[34] Y. Larring, T. Norby, Solid State Ionics 97 (1997) 523–528.
[35] S. Sorieul, S. Miro, M. Taillades-Jacquin, J. Dailly, F. Mauvy, M.-H. Berger, P. Berger, Nucl. Inst. Methods Phys. Res. B 266 (2008) 1430–1433.
[36] R. Hancke, S. Fearn, J.A. Kilner, R. Haugsrud, Phys. Chem. Chem. Phys. 14 (2012) 13971–13978.
[37] H. Mehrer, Diffusion in Solids, Springer Series in Solid State Science, Springer, Berlin and Heidelberg, 2007.
[38] J. Philibert, Atom Movements Diffusion and Mass Transport in Solids, Les Editions de physique, Les Ulis, 1991.
[39] M.E. Björketun, P.G. Sundell, G. Wahnström, D. Engberg, Solid State Ionics 176 (2005) 3035–3040.